Journal of Traffic and Transportation Engineering 14 (2026) 153-161
doi: 10.17265/2328-2142/2026.04.001

Evaluating Railway Vehicle Running Stability Based on Detection of the Three-Dimensional Center of Gravity

Kiwami Watanabe, Xian Chen and Yutaka Watanabe

Department of Logistics and Information Engineering, Tokyo University of Marine Science and Technology, Tokyo 135-8533, Japan

Abstract: Railway vehicle stability is an important factor affecting operational safety and ride quality. This study applies D3DCG (Detection of Three-Dimensional Center of Gravity) to evaluate the running stability of passenger railway vehicles without requiring prior knowledge of vehicle mass or spring stiffness. Field measurements were conducted on two commuter railway lines in the Greater Tokyo area, Japan using a motion sensor installed inside operating vehicles. After vertical acceleration and roll angular velocity measurements were taken during service operation, data were analyzed using FFT (Fast Fourier Transform) to extract dominant vibration frequencies. The obtained natural frequencies were substituted into the D3DCG equations to estimate the vehicle center of gravity height and the corresponding critical center of gravity position (L_{max}), which were used as rollover stability indicators. The estimated center-of-gravity positions were generally distributed within a physically reasonable range relative to the vehicle structure. Furthermore, an interesting tendency was observed in the calculated L_{max} values: the values initially decreased and subsequently increased along the measured sections. This tendency suggests that the stability margin of railway vehicles might vary depending on running conditions and vibration characteristics. The findings indicate that D3DCG-based analysis can provide a practical approach for evaluating railway vehicle stability using operational vibration data without requiring direct structural measurements.

Key words: D3DCG, center-of-gravity estimation, railway vehicle, running stability.

1. Introduction

Railway safety, particularly when vehicles enter curves at excessive speeds, remains an important concern. The 2005 Fukuchiyama line derailment, which caused more than 100 fatalities, is a stark reminder that overspeeding at curves can lead to catastrophic rollover accidents [1]. Although two decades have passed since that incident, overspeed remains a non-negligible issue affecting daily operations. Recent reports from the Ministry of Land, Infrastructure, Transport and Tourism [2] describe that overspeeding accounted for approximately 30% of all reported abnormal driving events in Japan's railway networks during 2021-2025. These figures suggest that speed-related risks persist, and that proactive monitoring of vehicle stability remains relevant today.

The D3DCG (Detection of Three-Dimensional Center of Gravity) theory, developed originally for maritime container trailers and later adapted to land vehicles, offers a promising approach to this problem [3-5]. Unlike conventional methods that require precise knowledge of vehicle mass and spring stiffness, the D3DCG theory derives the COG (center of gravity) height solely from the heave and roll frequencies measured during running. This feature makes it particularly attractive for operational monitoring, where mass and spring properties often vary or where they are difficult to obtain in real time.

Earlier studies conducted in the authors' laboratory [6, 7] applied the D3DCG theory to railway vehicles and thereby tracked COG shifts caused by passenger load variations and identified degradation of primary suspension springs over time. However, these earlier works specifically examined the COG position itself. They did not systematically address the two distinct

Corresponding author: Yutaka Watanabe, Doctor of Engineering, Specially Appointed Professor, research fields: the Detection of Three-Dimensional Center of Gravity.

rollover mechanisms which can occur in practice: (a) rollover attributable to loss of spring restoring force, and (b) rollover attributable to geometric instability when the vehicle tilts beyond its structural support limit, even with functional springs. The latter mechanism is particularly relevant to overspeed conditions, as the Fukuchiyama accident illustrates.

For the present study, we extend the D3DCG framework specifically for passenger railway vehicles by (i) redefining the effective spring width to include track-rail coupling, (ii) estimating COG heights from field running data on E231 series trains of East Japan Railway Company (JR East), and (iii) evaluating running stability using both the spring-based and geometric rollover limits. We further apply the proposed model to reconstruct the Fukuchiyama accident conditions, consequently verifying whether the calculated stability indices are consistent with the actual overspeed-induced rollover. Our goal is to provide a practical, real-time stability assessment tool that can help detect abnormal running conditions and which can support track maintenance decisions without requiring complex onboard instrumentation.

2. Methodology

2.1 Basic Concepts of D3DCG

The D3DCG [5], which was devised to prevent overturning of maritime container trailers, is based on the principles of ship buoyancy.

The figure above illustrates the application of the principles of this vessel to a land-based system. The

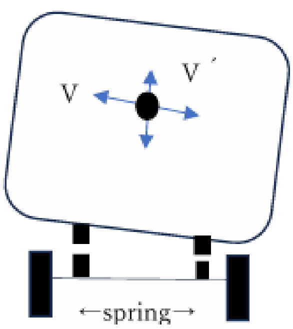

Fig. 1 Land mobility.

land-based vehicle is supported by an elastic structure and is subject to disturbances from the ground while in motion. As a result of these disturbances, natural vibrations occur around its COG (center of gravity), just as they do in a vessel floating on water. As shown in Fig. 1, it continues to oscillate with vertical frequency V' and lateral rolling frequency V.

The formula for calculating the center of gravity, L, of a moving body is given below [5].

$$L^2 + \frac{g}{4\pi^2 V^2} L - \frac{b^2 V'^2}{4V^2} = 0 \qquad (1)$$

In that equation, b represents the width of the left and right elastic structures supporting the moving body, g represents the acceleration because of gravity, and π represents the mathematical constant pi. A key feature of the three-dimensional center-of-gravity detection theory is that the center of gravity can be derived even without knowing the mass or the spring constant. Furthermore, for an object on the elastic structure, raising its center of gravity causes it to become increasingly unstable. The limit position of the center of gravity in a stationary state that can withstand this instability is defined as L_{max}. Using V', L_{max} is given [5] as presented below.

$$L_{max} = \frac{\pi^2 V'^2 b^2}{g} \qquad (2)$$

As shown in Eq. (2), the limit value for the center of gravity can be derived once the longitudinal vibration frequency is known. By comparing this limit value L_{max} with the center of gravity L, it is possible to ascertain the conditions under which the vehicle remains stable without rolling over.

2.2 Principle of Roll Over

To prevent a moving body from overturning while travelling in a straight line [6], the center of gravity limit L_{max} must always be higher than the center of gravity L. In this case, to cause the moving body to overturn, the difference in potential energy between L and L_{max} must be eliminated. Now, if the moving body is rotated in the lateral rolling direction, then it will reach a certain angle (defined as θ_{max}), at which point it loses its restoring force and overturns. This restoring force is, in fact, the spring energy supporting the moving body from both sides. The relation between potential energy and spring energy is given by Eq. (3).

$$mg(L_{max} - L) = \frac{1}{2}k\left(\frac{b}{2}\sin\theta_{max} + \frac{b}{2}\sin\theta_{max}\right)^2 \quad (3)$$

Here, m represents the mass of the moving body; k represents the spring constant of the elastic structure. Furthermore, by rearranging Eq. (3), θ_{max} can be expressed in terms of L and L_{max}.

$$\theta_{max} = \sqrt{\frac{L_{max} - L}{L_{max}}} \quad (4)$$

When a force is applied to a moving body from the side, it causes the body to tilt. At this point, the roll moment and the restoring moments from the left and right elastic structures act in opposition, as expressed mathematically in Eq. (5).

$$Lf = -m\left(\frac{kb^2}{2m} - gL\right)\sin\theta \quad (5)$$

The lateral external force is expressed in terms of the ratio q to gravitational acceleration. When formulated, this becomes Eq. (6).

$$f = mgq\cos\theta \quad (6)$$

One can rearrange Eqs. (5) and (6) to express q.

$$q = -\left(\frac{L_{max}}{L} - 1\right)\tan\theta \quad (7)$$

When $\theta = \theta_{max}$ and $q = q_{max}$, one obtains

$$q_{max} = -\left(\frac{L_{max}}{L} - 1\right)\tan\theta_{max} \quad (8)$$

At this point, q_{max} represents the external force beyond the rollover limit in terms of the elastic structural strength of the moving body. By expressing this in terms of Eq. (4), Eq. (8) can be written as shown below.

$$q_{max} = -\left(\frac{L_{max}}{L} - 1\right)\tan\left(\left(\sqrt{\frac{L_{max} - L}{L_{max}}}\right)\right) \quad (9)$$

The series of derivations presented up to this point has demonstrated that a moving body will overturn when an external force exceeding the restoring force of the elastic structure supporting it is applied. There is another type of rollover phenomenon distinct from that caused by the restoring force. The center of gravity might roll about a line connecting the center of gravity to the edge of the moving body, known as the roll radius. For this type of rollover, the restoring force is assumed to be sufficient: excessive speed might be the cause. Here, if the angle between the perpendicular from the center of gravity and the roll radius is denoted as ϕ, then the result is given by Eq. (10).

$$\tan\phi = \frac{b/2 - L\sin\theta}{L\cos\theta + h} \quad (10)$$

Here, h denotes the height from the point of contact with the road surface to the position of the vehicle's axle. If we derive the rollover limit condition using the moment caused by an external force that attempts to roll the center of gravity in the direction of the tangent to the center of gravity's trajectory, and the moment caused by gravity that attempts to return the center of gravity to its original position, then the result is given as Eq. (11).

$$mqg\cos\phi \geq mqg\sin\phi \quad (11)$$

Consequently, once a value of q is found that satisfies Eq. (11), the structural overturning limit is given by Eq. (12).

$$q_{\phi max} \geq \tan\phi_{min} \quad (12)$$

Therein, ϕ_{min} represents the roll angle at which the moving body reaches its geometric roll-over limit. From the above, and using Eqs. (10) and (12), the condition representing the geometric roll-over limit is given by Eq. (13).

$$q_{\phi max} \geq \frac{b/2 - L\sin[\tan^{-1}(-q\varphi max/((Lmax/L) - 1)]}{L\cos[\tan^{-1}(-q\varphi max/((Lmax/L) - 1)] + h} \quad (13)$$

2.3 Definition of the Train Springs

The rolling stock used in the experiment was the E231 series 0-subseries trains operated by JR East on the Joban and Narita Lines, as shown in Fig. 2 below [8]. The E231 series 0-subseries is a suburban commuter EMU (electric multiple unit) widely operated in the Greater Tokyo area. For this study, measurements were conducted with trains running between eastern Tokyo and northern Chiba Prefecture.

Regarding the test vehicles used for this center of gravity detection experiment, the bogies supporting the vehicles include components that can be interpreted as elastic structures. Fig. 3 portrays a side view of the bogie from the vehicle actually used for the experiment. In the figure, (1) denotes an axle spring; (2) denotes an air spring. In fact, the axle springs and air springs are installed respectively on the left and right sides of the vehicle body. Furthermore, the former is fitted to ensure running stability, whereas the latter is fitted to ensure ride comfort [7]. Although the center-to-center distance between the axle springs and air springs is not normally disclosed, this information was found at the National Diet Library [9]. The spring widths for each are presented below.

The D3DCG theory is based on the assumption that the natural oscillations of a moving object are measured. Consequently, because air springs might self-adjust, it is considered that they would dampen these natural oscillations. For this reason, air springs have been excluded from consideration in this study.

Whereas earlier research has specifically examined the elastic structures of rolling stock, this study incorporates consideration of the possibility that the track on which the rolling stock runs might also function as an elastic structure. Fig. 4 portrays a schematic diagram of this elastic support system. Item (3) represents the fastening spring, whereas Item (4) represents the track pad. Because track pads serve to reduce rail vibrations [10], it is conceivable that they act as elastic structures each time a train passes over them. Here, considering that trains run on rails, the width of the elastic structure in the track is expected to correspond to the track gauge, as shown in Fig. 3. If the train and the rails generate alternating vibrations, then this study treats the axle spring and the track gauge as a single unit to define the width of the elastic structure. This width, b, is presented below.

$$b = (Primary\ Width + Rail\ Width)\ /\ 2 \quad (14)$$

Fig. 2 Joban/Narita Line (Photograph by author).

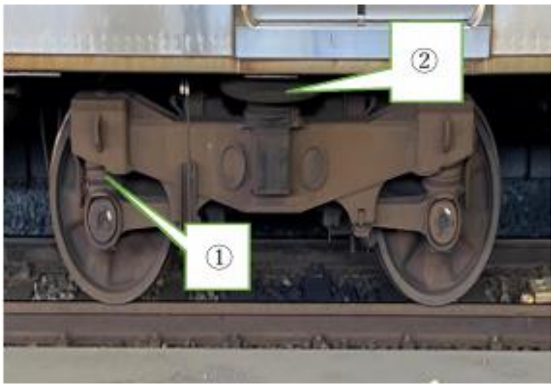

Fig. 3 Train springs (Photograph by author).

Table 1 Width between springs.

Primary spring	Air spring
1,700 mm	1,750 mm

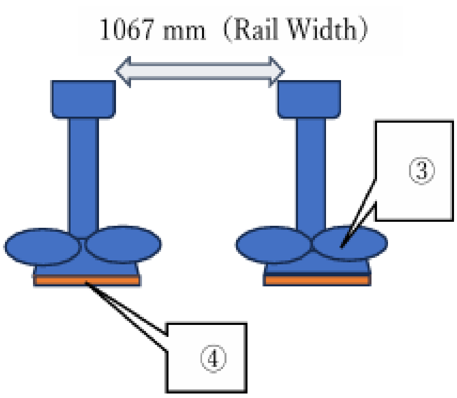

Fig. 4 Rail and springs.

3. Experiment of COG Detection on the Train

The following procedure was used for experimentation. First, after entering the vehicle, the laptop and motion sensor were connected via a cable, as shown in Fig. 5. To reduce measurement variation, the motion sensor position inside the vehicle was kept unchanged throughout all measurements. Next, the sensor was switched on. Measurements of vertical acceleration and angular velocity in the left-right direction were taken for two minutes.

It is necessary to confirm that the positive direction of the sensor's x-axis is the same as the direction of travel.

The measured vertical acceleration and roll angular velocity were transformed into the frequency domain using FFT (Fast Fourier Transform) analysis, as shown in Fig. 7. Because FFT analysis requires the number of samples to be a power of two, 2,048 samples were used for this study. Fig. 7 depicts the frequency spectra obtained from the measured motion data. Frequencies corresponding to the largest spectral amplitudes in the vertical and rolling directions were inferred as the dominant heave and roll frequencies of the vehicle. According to the D3DCG theory introduced in Chapter 2, these natural frequencies were subsequently substituted into Eqs. (1) and (2) to estimate the center-of-gravity position and evaluate running stability. For this experiment, the identified roll frequency was 0.488 Hz; the heave frequency was 1.46 Hz.

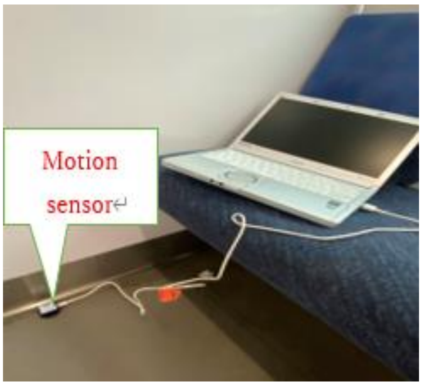

Fig. 5 Experiment situation (Photograph by author).

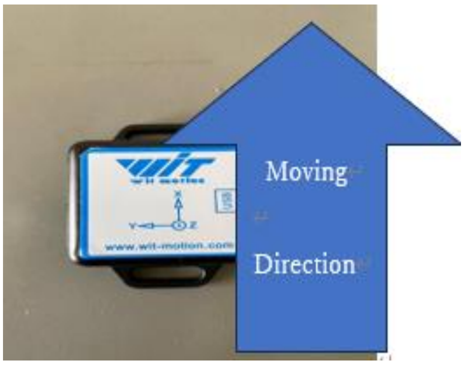

Fig. 6 Direction of the sensor.

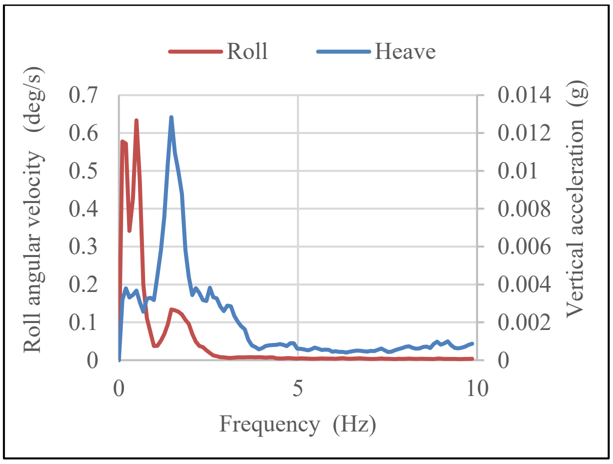

Fig. 7 Motion data.

4. Results and Discussion

Field experiments were conducted on the Joban Line (including the Abiko branch line) and the Narita Line, operated by East Japan Railway Company (JR East), in the Greater Tokyo area. These lines extend from eastern Tokyo to the northern part of Chiba Prefecture, approximately 20-60 km from central Tokyo. For this study, the term "section", defined as the track segment between two adjacent stations (i.e., an interstation section), is used hereinafter without further explanation. Measurements were taken of the following six consecutive sections: Kitasenju-Matsudo, Matsudo-Kashiwa, Kohoku-Araki, Kioroshi-Kobayashi, Kobayashi-Ajiki, and Ajiki-Shimosamanzaki. All measurements were performed with passengers in a seated posture.

Table 2 shows the center of gravity L and L_{max} for each section. As might be apparent from Table 2, the center of gravity varies from section to section. These

Table 2 Estimated center of gravity for each interstation section on the Joban/Narita Lines (Greater Tokyo area).

Number	Section	L (m)	L_{max} (m)
1	Kitasenju-Matsudo	1.65	4.08
2	Matsudo-Kashiwa	1.89	4.08
3	Kohoku-Araki	1.89	4.08
4	Kioroshi-Kobayashi	1.72	4.66
5	Kobayashi-Ajiki	1.81	3.54
6	Ajiki-Shimosamanzaki	1.97	4.66

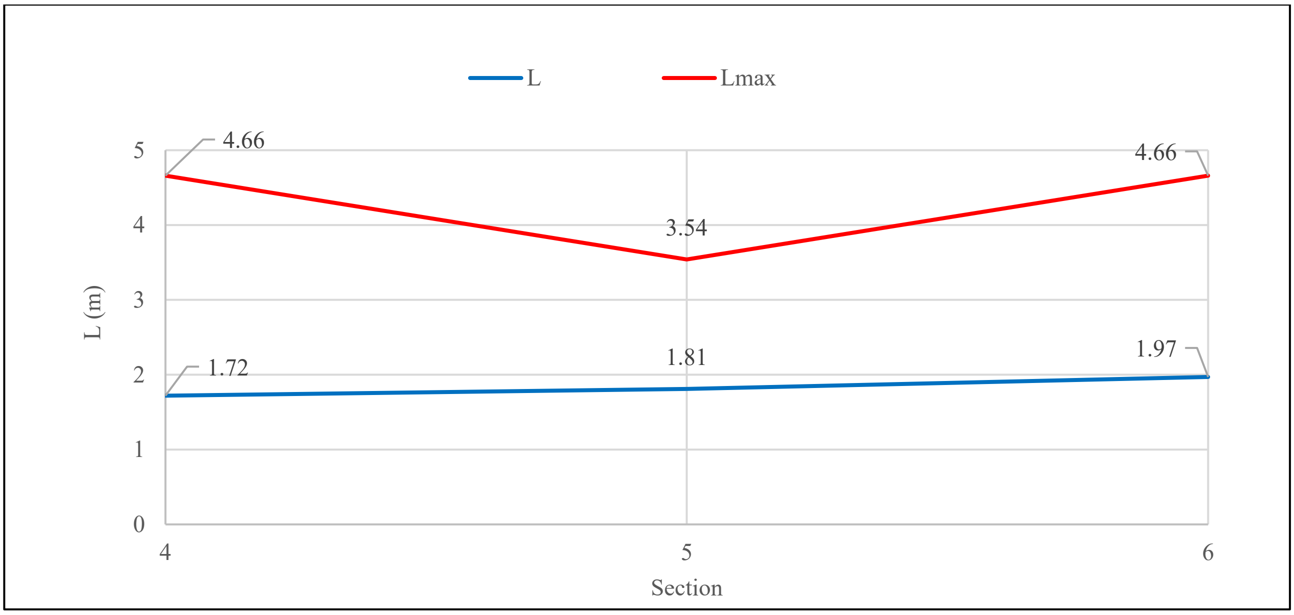

Fig. 8 Comparing L to L_{max} of Sections 4, 5 and 6.

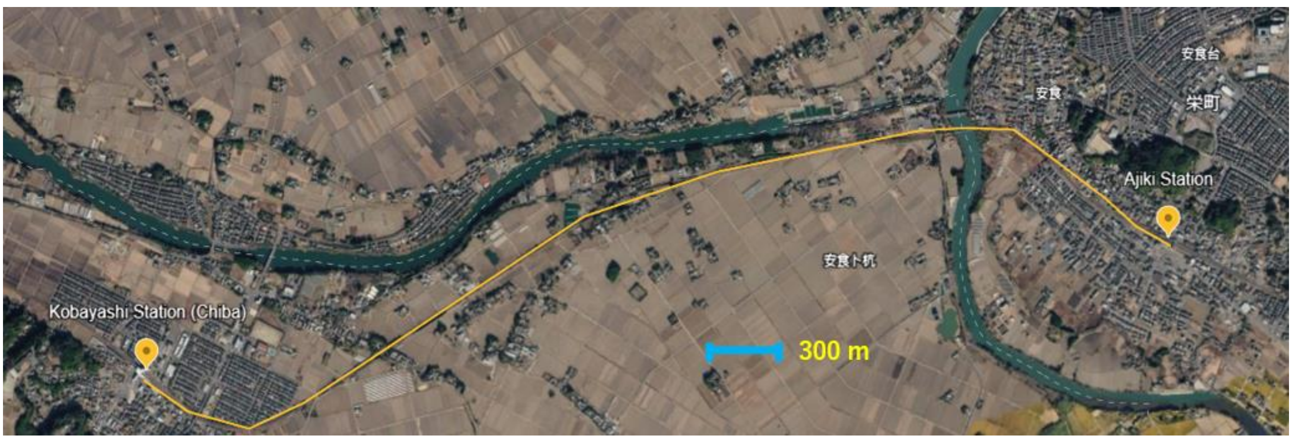

Fig. 9 Map of the Kobayashi-Ajiki section on the Joban/Narita Line, Greater Tokyo area. The railway line between the two stations is highlighted in yellow (Source: Google Earth).

variations in the center of gravity are thought to be attributable to passenger numbers, lateral sway on bends, or the influence of the elastic structure. According to the vehicle design drawings [11], the height from the top of the rail to the position corresponding to the lower edge of the vehicle's window frame is 1.965 m. Furthermore, because passengers were seated throughout all sections, the vehicle's center of gravity is thought to have varied according to each passenger's posture.

Table 3 L/L_{max} **for Sections 4, 5 and 6.**

Section	4	5	6
L/L_{max}	0.366	0.511	0.422

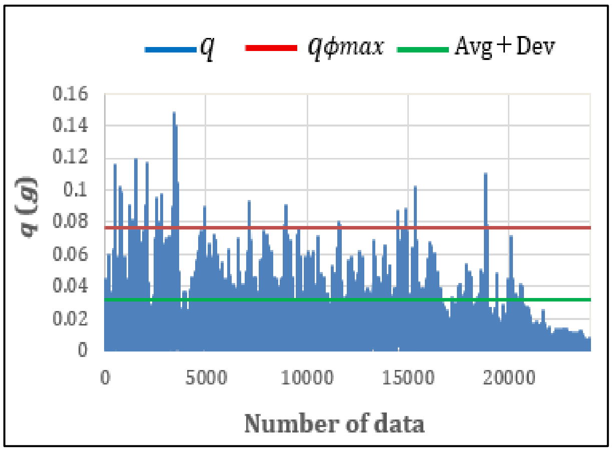

Fig. 10 Comparison of q **to** $q_{\phi max}$ **for the experiment sections.**

Fig. 8 shows selected data for L and L_{max} from three of the experiment sections. Fig. 8 shows that, whereas L_{max} was 3.54 m in Section 5 (Kobayashi-Ajiki), it was 4.66 m in Section 6 (Ajiki-Shimosamanzaki). Also, as described below, the ratio L/L_{max} is larger in Section 5 than in Section 6.

According to the theoretical framework presented in Chapter 2.2, L_{max} represents the limiting center of gravity height beyond which the spring restoring force can no longer maintain stability. As the actual center of gravity L approaches L_{max} (i.e., as the ratio L/L_{max} increases), the vehicle becomes increasingly unstable. By contrast, a decrease in L/L_{max} indicates an increase in the stability margin. In Section 5, $L/L_{max} = 0.511$, which is higher than in Section 6 (0.422), indicating that the stability margin in Section 5 is smaller. This result is consistent with the reduced L_{max} value observed in Section 5.

If the cause were attributable solely to the rolling stock, L_{max} would remain unchanged or decrease over time. Furthermore, as L_{max} is influenced only by longitudinal (heave) vibrations, the effects of factors such as curves are regarded as minimal. It is therefore thought that the track, which is defined as an elastic structure, might also be a contributing factor to the decrease in L_{max}. Consequently, these observations might reflect differences in the effective vibration characteristics of the vehicle-track interaction in Section 5, although direct evidence of track deterioration was not obtained in this study.

5. Comparing Experiment Sections to the Fukuchiyama Line Rollover Accident

The running stability was evaluated using the rollover principle outlined in Chapter 2. Although the rollover principle involves both q_{max} (spring-force limit) and $q_{\phi max}$ (geometric limit), we considered only $q_{\phi max}$ for the experiment sections. As discussed in Chapter 4, the ratio L/L_{max} in our experiment sections remained below 0.511, indicating that sufficient spring restoring force was available. Therefore, q_{max} was not the limiting factor; only $q_{\phi max}$ was evaluated. Furthermore, for $q_{\phi max}$, we took the track gauge as the width between the rail contact points and set height *h* from the point of contact with the top of the rail to the center of roll to zero.

The left-right acceleration q (denoted as lateral g) obtained from the sensors is expressed as positive or negative values depending on the direction. Because $q_{\phi \max}$ is an indicator of magnitude, the lateral acceleration data were converted to absolute values to facilitate comparison. Furthermore, sufficient amounts of data exist for evaluating driving stability. Therefore, assuming that the data are normally distributed, the mean and standard deviation were calculated and were used to compare the results with $q_{\phi max}$. Fig. 10 shows the relation between q and $q_{\phi max}$ over the experiment section. Here, sections for which the value of q exceeds $q_{\phi max}$ can be observed. The sway frequencies for each section are 0.488 Hz and 0.585 Hz, corresponding to periods of 1 to 2 s. However, because the time-series data are recorded at 0.005-s intervals, which is sufficiently short compared to the period length, it is considered unlikely that this would lead to a rollover. Consequently, the train did not exceed the speed limit. It was travelling stably.

The derailment accident which occurred on the Fukuchiyama Line in 2005 is attributed to excessive speed on a curve. Therefore, based on analytical data related to the accident [12], $q_{\phi max}$ was calculated by integrating it with the three-dimensional center of gravity detection theory. Here, the equations for excessive centrifugal acceleration α_y and the limit speed v can be expressed as shown below.

$$\alpha_y = \frac{v^2}{R} - \frac{c}{G}g \quad (15)$$

$$v = \sqrt{\left(\frac{c}{G} + \frac{G}{2h_G}\right)Rg} \quad (16)$$

In these equations, R represents the curve radius, c represents the cant, G represents the track gauge, and h_G represents the height of the vehicle's center of gravity above the top of the rail. Reportedly, at the time of the accident, the train entered a curve with a radius of 304 m at a speed of 116 km/h. Therefore, if we define the cant as 105 mm, which is the maximum for conventional lines, and set G = 1.067 m, then according to Eq. (15), the following is obtained.

$$\alpha_y = 2.45(m/s^2)$$

Consequently, the gravity ratio is q = 0.2501. Furthermore, because the apparent height of the center of gravity changes when the spring displacement is considered, if h_G in Equation (16) is increased by 25%, then h_G becomes 2.666432. Because h_G is the height of the center of gravity relative to the top surface of the rail, it coincides with L as defined in the three-dimensional center of gravity detection theory. Therefore, h_G was taken to be L as defined in the center of gravity detection theory. Furthermore, when considering the spring displacement, if q is set to q_{max} and calculated analytically, then L_{max} is given as the following.

$$L_{max} = 2.779956$$

In other words, $q_{\phi\max}$ at the time of the accident can be expressed as shown below.

$$q_{\phi max} = 0.072347$$

Based on the discussion presented above, a graph showing the relation between speed, q and $q_{\phi max}$ is shown in Fig. 11.

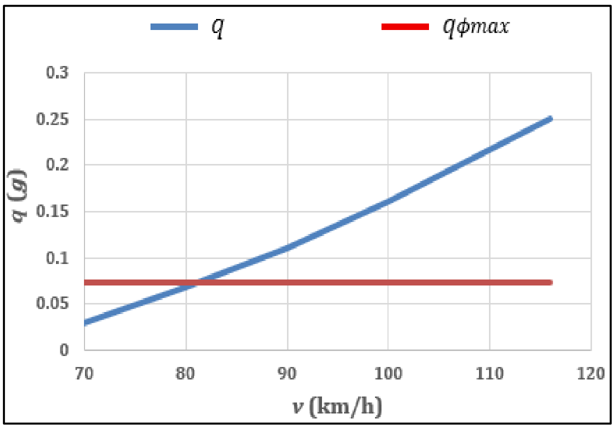

Fig. 11 Comparison of q to $q_{\phi max}$ for the Fukuchiyama accident reconstruction.

The speed limit at the scene of the accident on the Fukuchiyama Line is set as 70 km/h. Fig. 11 shows that, around 80 km/h, the value of q exceeds $q_{\phi max}$. It is therefore evident that, at 116 km/h, $q_{\phi max}$ is exceeded considerably. It is likely that, at this point, even applying the emergency brakes would have been too late. However, given the difference between L and L_{max} in the three-dimensional center of gravity detection theory, it is thought that some spring restoring force might still have been present at the time of the accident. Consequently, based on the value of $q_{\phi max}$, reconstructed D3DCG indicators were consistent with a geometric rollover scenario induced by excessive speed.

6. Conclusion

For this study, building on earlier research, we conducted experiments based on the width of elastic structures obtained through a literature review, and attempted to estimate the center of gravity of the vehicle. Challenges confronted for this study included the limited accuracy in identifying the experiment section and a lack of data. However, analyses of changes in the center of gravity position suggested not only that the rolling stock but also that the track acts as an elastic structure, potentially influencing changes in the center of gravity. Furthermore, specifically examining rollover mechanisms of two types with different causes, we evaluated running stability for the experiment section and the Fukuchiyama Line accident. The results confirmed that, overall, running was stable in the experiment section. By contrast, for the Fukuchiyama Line accident, the reconstructed D3DCG indicators were more consistent with a geometric rollover scenario ($q_{\phi max}$) than with a spring-induced rollover scenario (q_{max}).

Based on the discussion presented above, we conclude that continuous monitoring of changes in the center of gravity and evaluating running stability can be used for maintenance and inspection to achieve early track abnormality detection, and for preventing abnormal driving behaviors such as speeding.

References

[1] West Japan Railway Company. 2005. "Fukuchiyama Line Accident." https://www.westjr.co.jp/fukuchiyama/.

[2] Ministry of Land, Infrastructure, Transport and Tourism. 2026. "Abnormal Operation Report R3-R6." https://www.mlit.go.jp/tetudo/content/001898968.pdf.

[3] Kawashima, S. 2012. "Detecting Deterioration of Coil Spring for Railway Vehicle by the Three-Dimensional Detection of the Center of Gravity." *The Japan Society of Mechanical Engineers* 79 (803): 231-45.

[4] Kawashima, S., and Watanabe, Y. 2011. "Detection of the Center of Gravity on Moving Trains." *The Japan Society of Mechanical Engineers* 77 (778): 209-19.

[5] Watanabe, Y. 2017. "Dimensional Center of Gravity Detections for Preventing Roll Over Accidents of Trailer Trucks Hauling Containers." *Open Journal of Mechanical Engineers* 2 (1): 11-4.

[6] Yu, K., and Watanabe, Y. 2026. "Rollover Prevention Based on the Relation between Motion and Position of the Center of Gravity." *Journal of Traffic and Transportation Engineering* 14: 47-57.

[7] Primary Spring. 2017. *The Japan Society of Mechanical Engineers.* https://www.jsme.or.jp/jsme-medwiki/doku.php?id=20;1005079.

[8] Kotsu Shimbunsha. 2025. "E231 Series." *Railway Diagram Information*, pp. 38-40.

[9] The Japan Society of Mechanical Engineers. 1994. *Train Dynamics: Current Truck and Development Truck*, pp. 162-5.

[10] Railway Technical Research Institute. 2016. "Rail Pad." https://yougo.rtri.or.jp/dic/third_edition/detail.jsp.

[11] Ikaros Publications. 2025-2026. *Metropolitan Area Train New Series*, pp. 84-5.

[12] Matsumoto, Y., Sato, Y., Ono, H., and Mizuma, T. 2005. "Concepts and Preventive Measures for Derailment and Overturning Accidents. National Traffic Safety and Environment Laboratory." https://www.ntsel.go.jp/Portals/0/resource/forum/17files/17-19k.pdf.